Graefe's Arch Clin Exp Ophthalmol (1992) 230:561–568

Graefe's Archive
for Clinical and Experimental
Ophthalmology

Dysfunction of the blood-retina barrier following white light exposure

A tracer study with horseradish peroxidase and ferrous gluconate

Ruud Zweypfenning [1], Benedicte Putting [2], Gijs Vrensen [1], Jendo Oosterhuis [2], and Jaap van Best [2]

[1] Department of Morphology, The Netherlands Ophthalmic Research Institute, P.O. Box 12141, 1100 AC Amsterdam, The Netherlands
[2] Department of Ophthalmology, Leiden University Hospital, Leiden, The Netherlands

Received September 25, 1991 / Accepted April 8, 1992

Abstract. The aim of this investigation was to study the ultrastructural effects of white light on the retinas of pigmented rabbits. The retinas were exposed to white light (400–740 nm) at intensities between 65 and 140 mW/cm^2 for 1 h. Two days after exposure, the increased leakage of fluorescein measured with vitreous fluorophotometry could be mimicked on electron microscopy by the tracers ferrous gluconate and horseradish peroxidase (HRP). In cases of minimal fluorescein leakage, traces of HRP were found in the basal folds of the retina pigment epithelium (RPE). No HRP was observed apical to the tight junctions of the RPE cells. When there was a great amount of fluorescein leakage, HRP completely filled the RPE cytoplasm, the extracellular spaces, and several cells in the neuroretina. It is concluded that after exposure to low intensities of white light, blood-retina barrier dysfunction may be due to disruption of the RPE basal fold membrane, leading to increased transcellular passage. The intact tight junctions suggest the under these circumstances intercellular leakage is not a component of BRB dysfunction.

Introduction

It is generally accepted that there are three different mechanisms of light damage [8]: (1) mechanical light damage, such as that caused by the very intense light of YAG lasers (terrawatts/cm^2); (2) thermal damage (down to about 10 W/cm^{-2}) caused by a temperature rise to a point where proteins denature; (3) photochemical damage, in which the absorption of light by pigments does not lead to a significant temperature rise but to chemical reactions ending in the breakdown of cellular structures. This damage is probably the result of the production of singlet oxygen and free radicals, which are deleterious to the membranes [9].

In previous studies by Borsje et al. [3] and by Putting et al. [16], exposure levels of about 100 mW/cm^2 for 1–1.5 h were used to induce photochemical damage. These studies were carried out in rabbits using vitreous fluorophotometry for quantitative analysis of fluorescein leakage and pinpointed one of the photochemical effects at the BRB. Furthermore, it was demonstrated that white light can induce dysfunction of the BRB even at exposure levels below the threshold of ophthalmoscopically visible lesions. In the study by Putting et al. [16], it was found that in the range of 65–140 mW/cm^2 the fluorescein leakage into the vitreous increased exponentially with light intensity, starting at a value of 69 mW/cm^2. In the range of 65 to 89 mW/cm^2 (subthreshold range) no lesions were observed on fundus examination. In the threshold range (90–110 mW/cm^2), 11 out of 14 rabbits showed a lesion, while in the superthreshold range (111 to 140 mW/cm^2) all rabbits showed fundus lesions.

The first aim of the present study was to visualize the precise location of the BRB dysfunction at the RPE ultrastructurally, employing identical animals and a set-up identical to that used for the fluorophotometry study by Putting et al. [16]. Because fluorescein is not electron dense, the increased passage of fluorescein through the BRB was mimicked with two electron dense tracers: (a) ferrous gluconate (FG), which has a molecular size comparable to fluorescein (480 Da vs 500 Da) and (b) horseradish peroxidase (HRP) with a molecular weight of 40,000 Da. An additional aim of the study was to visualize the primary effects on the neuroretina.

Materials and methods

Twelve full-grown pigmented chincilla gray rabbits, weighing 2.5–3 kg were used for electron microscopic evaluation (2 were exposed to subthreshold irradiation, 5 to threshold irradiation and 5 to superthreshold irradiation). For a detailed description of the light-exposure procedure, the reader is referred to Putting et al. [16]. In short, the rabbits were kept in a light cycle with a daytime illumination of 150 to 400 lux. Retinas were exposed in vivo for 1 h to white light from a xenon arc lamp in the range of 65–140 mW/cm^2. Using specific filters, the wavelength range was restricted to 400–740 nm. The light spot of the xenon arc was projected onto the retina just below the myelinated nerve fibers in

Correspondence to: R. Zweypfenning

the visual streak of the retina. The alteration of the BRB was monitored with vitreous fluorophotometry (VF). The ratio of vitreous fluorescein concentration in the exposed eye to the control eye was used as a parameter for permeability. An increase in ratio after exposure indicates a dysfunction of the BRB. VF was performed several days before the light exposure and the second day after exposure. The electron-dense tracers were injected systemically in the experimental animals 60 min after VF. Depending on the tracer used, the animals were killed with an overdose of sodium pentobarbital after 20 or 60 min and both eyes were enucleated. The non-exposed fellow eyes of these rabbits served as tracer controls. Two experimental animals were killed 2 h after VF without tracer administration and served as non-tracer controls to study the effect of the tracer. The anterior segment of the eyes up to the ora serrata was removed to facilitate penetration of the fixative.

For electron microscopic visualization of the BRB dysfunction, two electron dense tracers were used: the first, FG, was injected intra-arterially in a dosage of 1 g/kg. After 60 min, the animals were killed with an overdose of sodium pentobarbital. The enucleated eyes were immersed for several hours in a cold (4° C) 0.1 M phosphate-buffered fixative containing 1.25% paraformaldehyde and 1% glutaraldehyde (pH 7.4). Samples of the exposed part of the retina and of corresponding sites in the contralateral control eye were dissected under a biomicroscope. After thorough rinsing in phosphate buffer, the retinal samples were postfixed with OsO_4, dehydrated and embedded in Epon 812. The second tracer was HRP. Twenty minutes after the intra-arterial injection of HRP (Sigma, type II) in a dosage of 200 mg/kg, the animals were killed with an overdose of sodium pentobarbital and the eyes were enucleated. The enucleated eyes were immersed for several hours in a cold (4° C) 0.1 M cacodylate-buffered fixative containing 1% paraformaldehyde and 1.25% glutaraldehyde (pH 7.4). After thorough rinsing in the cacodylate buffer, the pieces of retina were incubated for 30 min in 50 ml TRIS-HCl buffered solution (0.1 M, pH 7.6) containing 0.05% 3,3′-diaminobenzidine (Sigma) and 0.01% H_2O_2. In some samples, the diaminobenzidine reaction product was intensified with a gold-substituted silver peroxidase technique (GSSP technique) [22]. The retinal samples were postfixed with OsO_4, dehydrated, and embedded in Epon 812.

Ultrathin sections were stained with lead citrate and uranyl acetate and inspected in a Philips EM 201 transmission electron microscope. Light microscopic examination was carried out on semithin (1 μm) sections of the same material after staining with toluidine blue.

Results

Ophthalmoscopic results

Based on ophthalmoscopic examination, three irradiation ranges were determined: (1) 65–90 mW/cm^2 (subthreshold), with no ophthalmoscopically visible lesions; (2) 90–110 mW/cm^2 (threshold), in which most cases (79%) developed ophthalmoscopically visible lesions within 2 days after exposure; (3) 110–140 mW/cm^2 (superthreshold), in which most cases (60%) developed an ophthalmoscopically visible lesion within 1 day after exposure.

Histology

Retinas of control and irradiated animals that had received an injection of HRP or FG were carefully compared with retinas of non-injected animals, but neither HRP nor FG gave rise to any ultrastructural aberrations.

Control eyes

In control animals, an excess of HRP and FG was demonstrated in the choroid and Bruch's membrane (Fig. 1) and in the extracellular space between the RPE basal folds (Fig. 2) up to the junctional complex (Fig. 3). In the RPE cells, vesicles or tubular structures containing traces of HRP were incidentally observed. In the control retinas of animals not injected with HRP, coated vesicles were rarely observed (Fig. 4) and if seen at all, they were found preferentially at the nuclear region of the basal membrane (Fig. 5). No uncoated endocytotic vesicles were observed. The absence of uncoated vesicles is not artifactual, as adjacent capillary endothelial cells have numerous smooth endocytotic vesicles (Fig. 4). In the subretinal space, no evidence of the tracers was observed, indicating that the tracers had not reached the subretinal space either by a transcellular or by an extracellular pathway.

Exposed eyes

Subthreshold (65–89 mW). At exposures below 90 mW, no fundoscopic lesions were found, and the fluorescein leakage ratio remained below two. The retinas of control eyes and retinas exposed to white light appeared to have similar ultrastructural features. No indications of cellular alterations such as disturbed membranes of the receptor outer segments or swollen mitochondria were found in the exosed retinas. At this level of exposure, HRP and FG had the same distribution as in control eyes. With both HRP and FG, electron dense particles (FG or GSSP intensified HRP) or reaction product (HRP) were observed in the lumen of the blood vessels, extracellular to the vascular endothelium, and in Bruch's membrane. The tracers had diffused into the extracellular space between the RPE basal folds up to the junctional complex. No detectable amounts of tracer were observed in the subretinal space. As in controls, cytoplasmic vesicles containing HRP were extremely rare.

Fig. 1. Control retina after horseradish-peroxidase (HRP) injection (HRP-DAB). Electron-dense reaction product can be seen in the capillaries (*C*) of the choroid, Bruch's membrane (*B*) and between the basal folds (*BF*). *N*, Nucleus; *J*, junction complex; *O*, receptor outer segment. (Bar indicates 1 μm)

Fig. 2. Control retina after HRP injection (HRP-DAB-GSSP). *Arrowheads* indicate the intensified HRP-DAB particles in Bruch's membrane and in the extracellular space between the RPE basal folds. These particles are absent in the RPE basal fold cytoplasm. (Bar indicates 0.2 μm)

Fig. 3. Control retina after HRP injection (HRP-DAB-GSSP). HRP particles in the desmosomal part of the junction complex. (Bar indicates 0.5 μm)

Fig. 4. Control retina without tracer injection. The endothelial cell of the choriocapillaries (*E*) contains numerous smooth vesicles (*v*) while in the basal folds (*BF*) only very few coated vesicles (*c*) were observed. (Bar indicates 0.5 μm)

Fig. 5. Control retina without tracer injection. The region of the RPE cell nucleus (*N*) is where most of the vesicles (*c*) were found that were scarcely coated at all. The coated vesicles seem to fuse with smooth tubular elements (*arrow*). *B*, Bruch's membrane; *BF*, basal folds. (Bar indicates 0.2 μm)

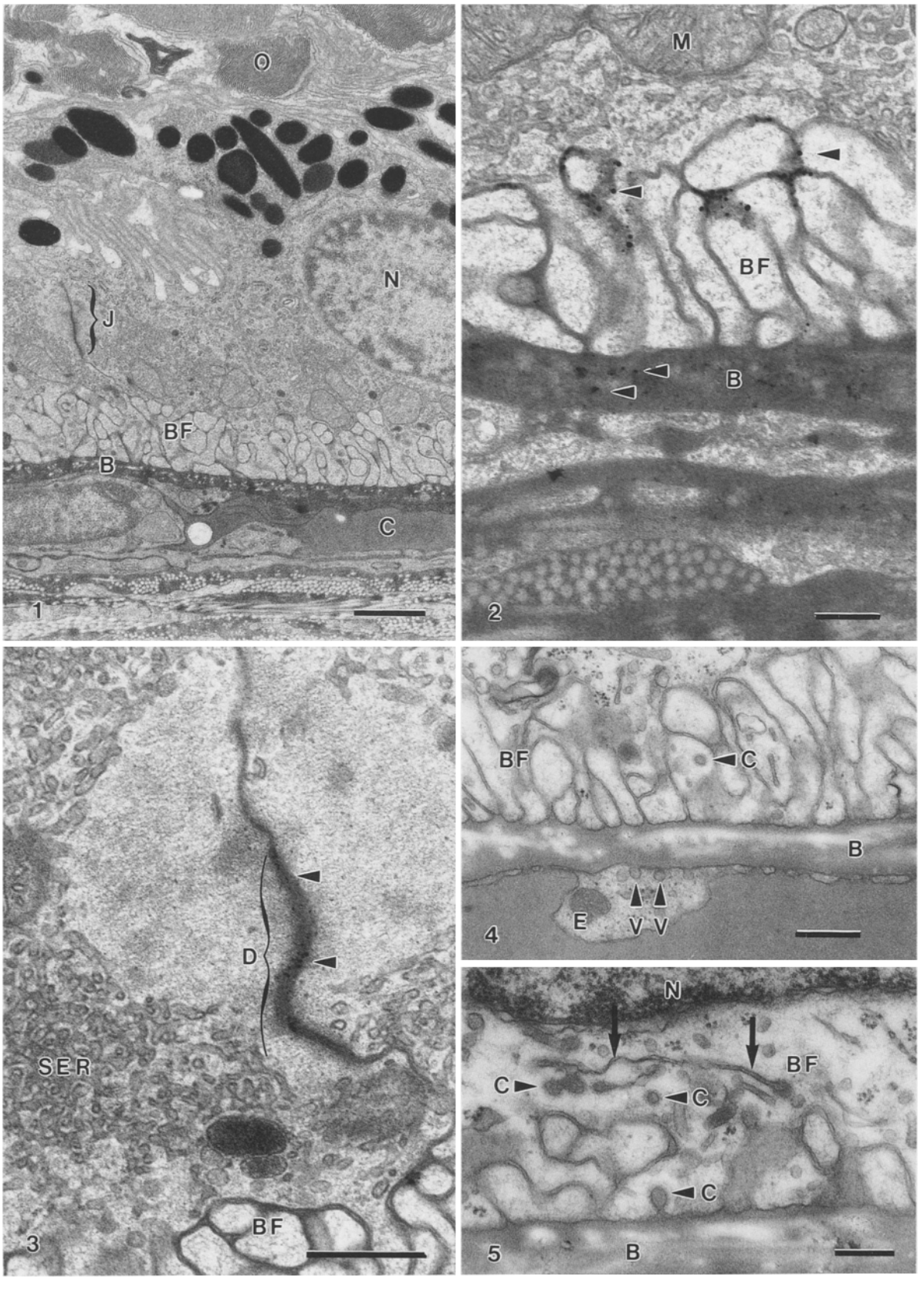
O
N
J
BF
B
C
1
M
BF
B
2
D
SER
BF
3
BF
C
B
E
V V
4
N
BF
C
C
C
B
5

Threshold and superthreshold (90–140 mW). The five rabbits exposed to threshold intensities (90–110 mW) showed an increase in VF ratio of 2 to 40. All the rabbits exposed to superthreshold intensities (110–140 mW) showed VF ratios of 14 or more. With VF ratios higher than 8, an excessive amount of HRP could be demonstrated in the subretinal space. Radial sections were cut taking into consideration the fact that the intensity of the exposure decrease towards the periphery of the irradiated retinal area. We expected a difference in histological damage to the periphery as compared to the center of the spot.

After exposures in the threshold range (90–110 mW/cm^2 for 1 h), the histology of exposed retinas (when no electron dense tracer was injected) showed no obvious ultrastructural alterations. However, analogous to the fluorophotometric evaluation, excessive leakage could be traced at the EM level with HRP and FG. The most interesting observations were made at the periphery of the lesion. In this region, the first signs of increased HRP uptake were observed when the GSSP procedure was applied. The first indications of malfunction of the BRB were small amounts of tracer located in the cytoplasm in the region of the RPE basal folds (Fig. 6) and sometimes at a short distance from the basal folds in vesicles of the smooth endoplasmatic reticulum (Fig. 7). Side the control experiments, the HRP was able to diffuse between the RPE cells in the direction of the subretinal space, but the diffusion was still obstructed by the tight junctions (Fig. 8). In the periphery, no ultrastructural changes were found in the neuroretina.

In the center of the lesion, HRP completely filled the cytoplasm of the RPE cells (Fig. 9). In addition, HRP reaction products were found in the extracellular space of the neuroretina (Fig. 9). The tight junctions seemed to be ultrastructurally intact. However, due to the masking effect of the HRP in the cytoplasm, it was not possible adequately to judge the passage of HRP at the tight junction.

In the superthreshold range (110–140 mW/cm^2/h), ultrastructural damage became obvious. The RPE cells showed increasing degradation, membranes of outer segments were disturbed, and other components of the retina were also affected. Nearly all HRP had leaked out from Bruch's membrane and the RPE cells, while the extracellular space (Fig. 11) and some cells in the neuroretina were completely filled with HRP. The cells stained with HRP could be identified as Müller, photoreceptor, and amacrine cells (Figs. 12–14). Most of the HRP-filled receptor cells had comparable ultrastructural characteristics: a short outer segment and an ellipsoid situated between the outer segments of rods, while the triangular pedicles showed two or more synaptic ribbons.

The FG particles, being smaller then HRP particles, were harder to detect with EM, but in principal this tracer yielded the same results as HRP. In the threshold range, a transcellular movement of FG in the direction of the subretinal space was observed (Fig. 10) while the extracellular diffusion seemed to be obstructed by the ultrastructurally intact tight junctions.

Discussion

Methodological considerations

In this study the white-light-induced BRB dysfunction, quantified in vivo with VF, was visualized with HRP and FG. It was expected that FG, which has a small molecular size comparable to that of fluorescein, would give the best insight into the initial manifestations of BRB breakdown. However, it was discovered that the electron-dense particles were too small and the tracer detectable only when clumps of particles were present. This necessitated administration of a large dose of the tracer. It is also possible that the large dose was needed because of clearance of the FG from the bloodstream by erythrocytes and liver cells. Although the use of FG was limited, it also demonstrated that BRB disruption leads to a transcellular flow to the neuroretina. HRP gave much clearer results. Without the GSSP procedure, leakage could be detected at a ratio of 8. When the GSSP procedure was used, signs of leakage could be detected at the rim of the field of illumination. As there was a strong decrease in irradiation towards the rim, the fluorescein leakage mimicked at these sites must have a ratio far below 8.

Intercellular leakage

Theoretically, the main pathways for leakage of macromolecules from the choriocapillaries to the subretinal space are an intercellular route through the junctional complexes between the RPE cell or a transcellular route through the RPE cells. An intercellular route would mean that the sealing part of the junctional complexes between the RPE cells, i.e., the tight junctions, would become permeable for molecules. Normally, the tight junctions seal neighboring cells together to create a continous barrier between cells across which even small molecules and ions are unable to pass [2]. When a minimal dysfunction was indicated electron microscopically by increased HRP presence in the RPE cytoplasm, we were

Fig. 6. Peripheral lesion of retina after threshold illumination (HRP-DAB-GSSP). Gold-silver grains (*arrowheads*) are present in the Bruch's membrane (*B*) and in the cytoplasm of the RPE basal folds (*BF*). *C*, capillary. (Bar indicates 0.2 μm)

Fig. 7. Peripheral lesion of retina after threshold illumination (HRP-DAB-GSSP). Gold-silver grains (*arrowheads*) are present in smooth endoplasmatic reticulum near the RPE basal folds. (Bar indicates 0.2 μm)

Fig. 8. Peripheral lesion of retina after threshold illumination (HRP-DAB-GSSP). Gold-silver grains (*arrowheads*) are present in the desmosomal part (*D*) of the junctional complex. In the gap junctional and tight junctional part (*GT*) and the subretinal space (*S*), no traces of HRP are observed. The melanin granules (*Me*) give always a gold-silver reaction. (Bar indicates 0.2 μm)

Fig. 9. Threshold lesion (HRP-DAB). The HRP completely fills the cytoplasm of the RPE cells (*R*). The extracellular spaces between the outer segments are also filled with HRP (*arrows*). *L*, lipofuscin; *O*, receptor outer segment. (Bar indicates 1 μm)

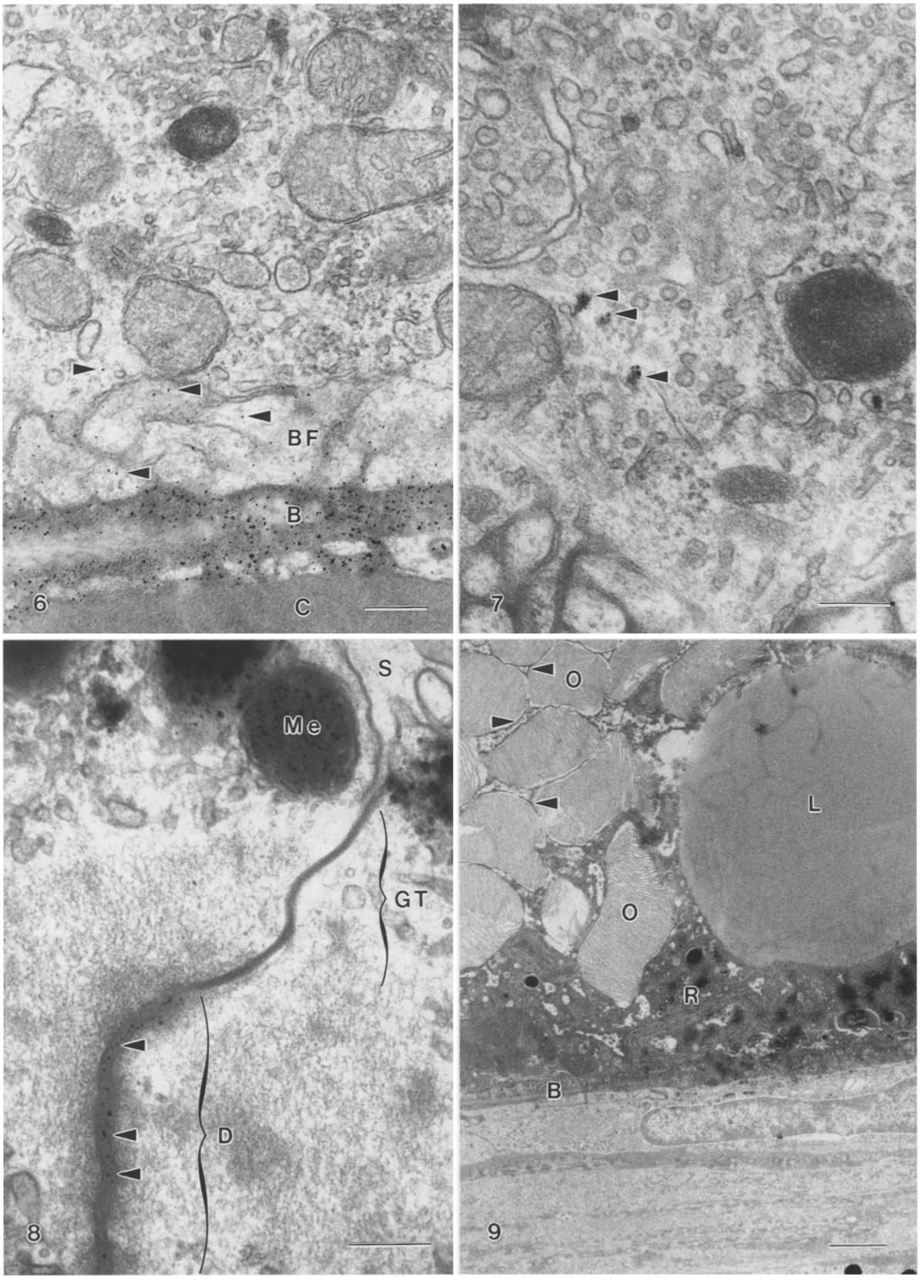
BF
B
C
6
7
S
Me
GT
D
8
O
L
O
R
B
9

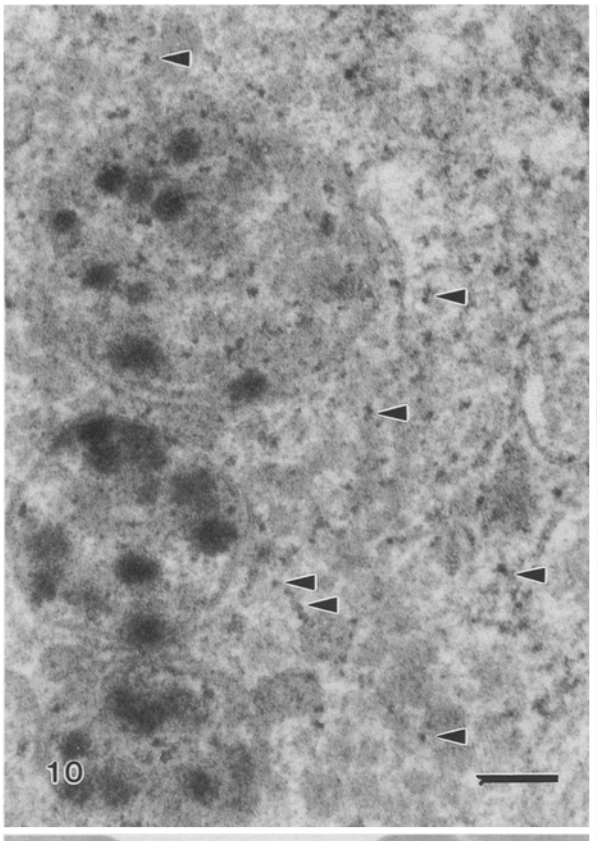
10

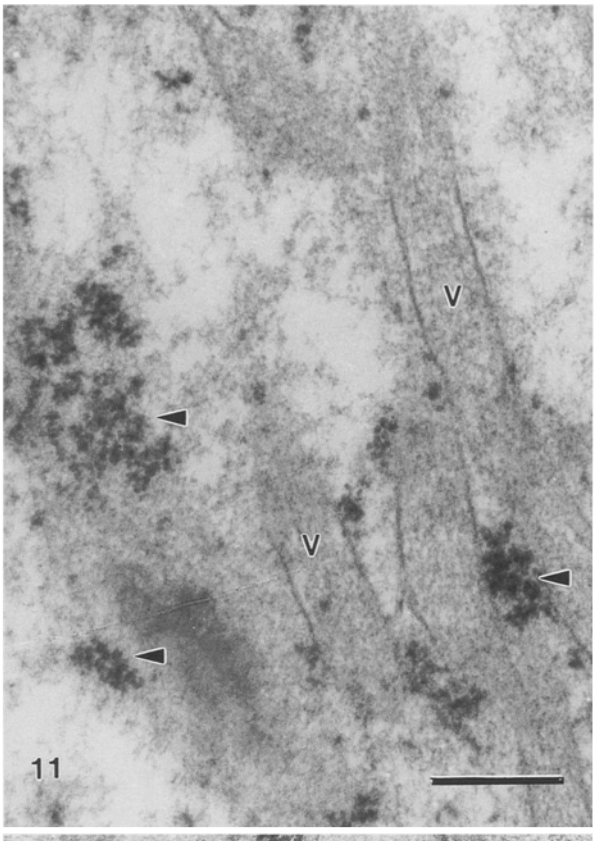
V
V
11

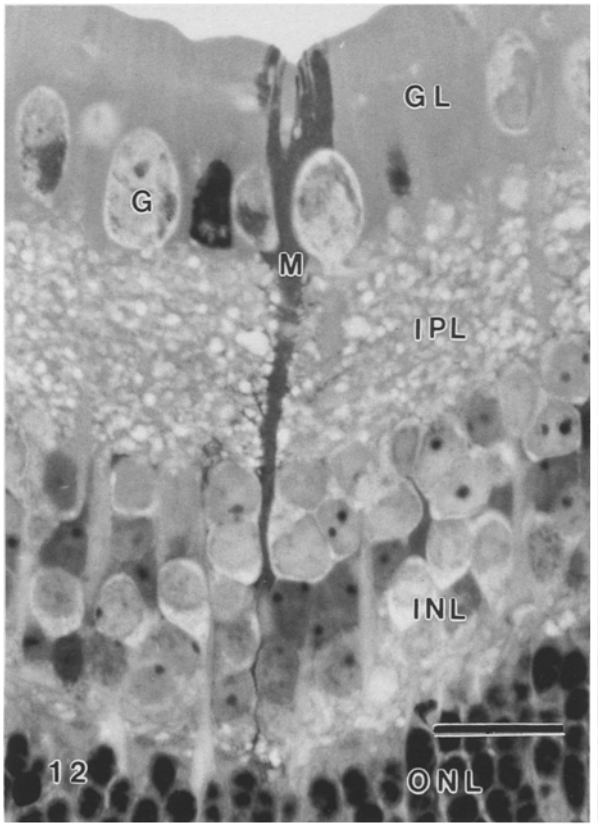
GL
G
M
IPL
INL
ONL
12

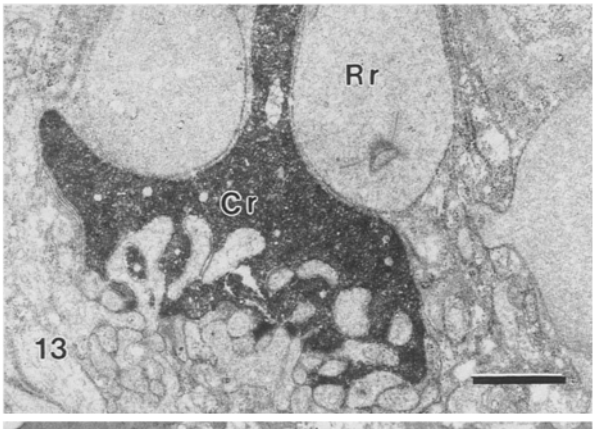
Rr
Cr
13

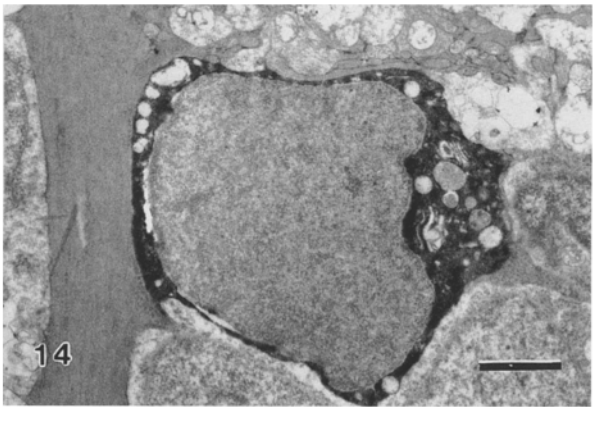
14

unable to detect any traces of HRP in the subretinal space or the intercellular space apical to the tight junction. This indicates that the tight junctions were still effective non-leaky barriers between the RPE cells.

Because the tracer had reached the subretinal space and had further diffused randomly into the neuroretina and the extracellular space in the apical region of the RPE at higher irradiation levels, it was difficult to exclude some leakage through the tight junctions. However, even in these cases, the tight junction remained intact electron microscopically, and no tracer was found at the tight junctional sites, indicating that intercellular leakage is not a component of the BRB dysfunction.

Transcellular leakage

Macromolecules can cross cellular membranes by endocytosis. Depending on the characteristics of the molecule, it can be bound to coated pits on the membrane and endocytosed in coated vesicles (adsorptive or receptor-mediated endocytosis), or it can be passively engulfed with the fluid of smooth vesicles (bulk-phase endocytosis). Receptor-mediated endocytosis is a selective concentrating mechanism enabling the ingestion of large amounts of specific ligands (e.g., low-density lipoproteins) without taking in a correspondingly large volume of extracellular fluid [2]. Bulk-phase endocytosis is a non-selective transport. When the vesicles are formed, part of the extracellular fluid with its molecular contents such as HRP is passively ingested and surrounded by a membrane. The vesicles enter the intracellular space and fuse with lysosomes. The HRP is further transported by preformed vesicles or elements of the smooth endoplasmatic reticulum [6, 7, 18]. Essential in both pathways is that the HRP be segregated from the cytoplasm into membrane-delimited organelles. This is in contrast with the uptake of HRP in damaged cells, e.g., mechanical disruption of the axonal membrane of neurons by local freezing or the passage of concentrated inotophoretic current may provide the conditions necessary for direct axoplasmic entry of HRP [10, 15]. At the site of the injury, the labelling is diffuse, but at some distance from the injury, the HRP becomes segregated from the cytoplasm into membrane-delimited organelles [1, 11].

The main observations in this study concerning the basal RPE membrane and uptake of HRP are: (a) in non-damaged, non-HRP-treated retinas, endocytotic vesicle formation in the basal membrane region is rare, and only coated vesicles were encountered; (b) in non-damaged, HRP-treated retinas, the cytoplasm was free of HRP, and very few vesicles and tubular structures contained HRP although there was an excess of HRP present in the extracellular space of the basal folds and in the intercellular space up to the tight junctions; (c) after exposures causing minimal dysfunction, in addition to the scarce HRP-filled vesiclelike structures, diffuse traces of HRP not enveloped by membranes were found in the cytoplasm of the RPE basal folds. In contrast to most other epithelial linings studied [2], HRP is extremely scarce in the RPE cell bodies under normal physiological circumstances, demonstrating that bulk phase endocytosis must be extremely rare. Some HRP enters the cell with adsorptive endocytosis mediated by coated vesicles. This means that in the RPE, non-selective uptake of macromolecules does not take place or is extremely rare. This protects the neuroretina and RPE cells from an uncontrolled influx of macromolecules and toxic substances and thus meets the criteria of a barrier. However, this does not affect the uptake of nutrients and ions since most of these are internalized by specific membrane channels.

After exposures causing minimal BRB dysfunction, diffuse traces of HRP not enveloped by membranes were found in the cytoplasm of the RPE basal region. This indicates that light has damaged the membrane, which becomes leaky, resulting in an uncontrolled diffusion. Delmelle [4] has proposed that light damage to the retina is due in part to singlet oxygen, and Lion et al. [13] have detected singlet oxygen in irradiated retinas. The most destructive role of singlet oxygen lies in the peroxidation of polyunsaturated lipids composing the major constituents of the membrane structure [8]. Thus, at threshold and superthreshold level, singlet oxygen is a good candidate for RPE cell membrane destruction. The results of other investigators who found RPE cells with ultrastructurally intact tight junctions after exposures at threshold level [3] or in an edematous RPE in mildly damaged areas [20] support our findings of a transcellular leakage. In rod-dominated retinas, the RPE cells are sensitive to extracellular K^+ concentration changes and behave like K^+ electrodes [5]. The RPE membrane potential changes give rise to the C-wave in the electroretinogram [14, 19]. Disruption of the RPE membranes should lead to disturbance of the RPE membrane potentials and thus to disappearance of the C-wave.

Direct light damage to parts of the neuroretina

Except for conelike receptors, no ultrastructural changes were found in irradiated retinas in the threshold range, e.g., no swollen mitochondria or disturbed membranes of outer segments were observed. Nevertheless, there

Fig. 10. Threshold lesion (FG). Ferrous gluconate precipitations (*arrowheads*) in the cytoplasm of RPE cells after threshold irradiation. (Bar indicates 0.1 μm)

Fig. 11. Threshold lesion (HRP-DAB). HRP in the extracellular spaces between receptor ellipsoids and Müller cell villi (*V*) and on the outer nuclear layer side of the outer limiting membrane between the nuclei of the outer nuclear layer. (Bar indicates 2 μm)

Fig. 12. Threshold lesion (HRP-DAB). Light microscopic overview of the retina with a HRP filled Müller cell (*M*). *G*, Ganglion cell; *GL*, ganglion layer; *IPL*, inner plexiform layer; *INL*, inner nuclear layer; *ONL*, outer nuclear layer. (Bar indicates 20 μm)

Fig. 13. Threshold lesion (HRP-DAB). Cone receptor pedicle (*Cr*) filled with HRP. *Rr*, Rod receptor pedicle. (Bar indicates 1 μm)

Fig. 14. Threshold lesion (HRP-DAB). HRP-filled amacrine cell in the inner nuclear layer of the neuroretina. (Bar indicates 2 μm)

were other indications of damage. When the BRB was damaged and HRP was administered, the HRP filled not only the whole extracellular space in the retina, but was also found intracellularly in different cell types (receptor, Müller, and amacrine cells) in the neuroretina. In the HRP-filled receptor and Müller cells, the HRP was not segregated from the cytoplasm into membrane-delimited organelles, but was diffusely distributed in the cytoplasm. The number of cells filled with HRP increased with the irradiation level. This points more in the direction of direct light damage to components of the neuroretina than an endocytotic uptake of HRP. Furthermore, just as with RPE cells, the inward flow of HRP points to a direct effect on the membrane.

As mentioned above, all HRP-filled receptor cells had ellipsoids situated between the outer segments of other receptors, triangular pedicles containing several synaptic ribbons, and nuclei situated directly against the outer limiting membrane. These characteristics indicate that they are cone receptor cells. In experiments in which no tracer was administered, only these receptors showed swollen mitochondria. Müller cells are important for retinal maintenance and signal conductance of neural cells [17]. It is imaginable that malfunction of the Müller cells leads to secondary damage in the neuroretina.

Kremers and van Norren [12] have proposed two classes of photochemical damage. Class I is found at low-irradiation levels (1 mW/cm^2) over rather long periods (several hours to weeks). Shortly after exposure, the damage is mainly restricted to the photoreceptors. Class II damage is found with high light levels (>10 mW/cm^2) over shorter periods (up to 4 h). Shortly after exposure, the damage is mainly restricted to the retinal pigment epithelium. Since we used intensities ranging from 65–140 mW/cm^2 for 1 h, the damage should belong to class II. Indeed, damage is mainly restricted to the RPE layer, while the neuroretina seems hardly to be affected. However, after an evaluation with HRP, several cell types show an aberrant uptake of HRP, indicating that their membranes, just like RPE membranes, may be functionally altered.

Acknowledgements. The authors would like to thank N.C.M. Bakker and L. van Sint Annaland for photographic assistance. This research project was funded by the "Haags Oogheelkundig Fonds."

References

1. Adams JC, Warr WB (1976) Origins of axons in the cat's acoustic striae determined by injection of horseradish peroxidase into severed tracts. J Comp Neurol 170:107–122
2. Alberts B, Bray D, Lewis J, Raff M, Roberts K, Watson JD (1989) Molecular biology of the cell. Garland, New York London
3. Borsje RA, Vrensen GFJM, Van Best JA, Oosterhuis JA (1990) Fluorophotometric assessment of blood-retinal barrier function after white light exposure in the rabbit eye. Exp Eye Res 50:297–304
4. Delmelle M (1978) Retinal sensitized photodynamic damage to the liposomes. Photochem Photobiol 28:357–360
5. Dowling JE (1987) Electroretinogram and glial responses. In: the retina, an approachable part of the brain. Belknap Press of Harvard University Press, Cambridge, Mass, London, pp 164–186
6. Droz B (1973) Renewal of synaptic proteins. Brain Res 62:383–394
7. Droz B, Rambourg A, Koenig HL (1975) The smooth endoplasmatic reticulum: structure and role in the renewal of axonal membrane and synaptic vesicles by fast axonal transport. Brain Res 93:1–13
8. Ham WT Jr, Müller HA, Ruffolo JJ Jr, Millen JE, Cleary SF, Guerry RK, Guerry D (1984) Basic mechanisms underlying the production of photochemical lesions in the mammalian retina. Curr Eye Res 3:165–174
9. Handelman GJ, Dratz EA (1986) The role of antioxidants in the retinal pigment epithelium and the nature of peroxidant-induced damage. Adv Free Radical Biol Med 2:1–89
10. Herkenham M, Nauta WJH (1977) Afferent connections of the habenular nuclei in the rat. A horseradish peroxidase study, with a note on the fiber-of-passage problem. J Comp Neurol 173:123–146
11. Holländer H, Vanegas H (1977) The projection from the lateral geniculate nucleus onto the visual cortex of the cat: a quantitative study with horseradish peroxidase. J Comp Neurol 173:519–536
12. Kremers JJM, Van Norren D (1988) Two classes of photochemical damage of the retina. Lasers Light Ophthalmol 2:41–52
13. Lion Y, Delmelle M, Van den Vorst A (1976) New method of detecting singlet oxygen production. Nature 263:442–443
14. Oakley B II, Steinberg RH, Müller SS, Nilson SE (1977) The in vitro frog pigment epithelium cell hyperpolarization in responses to light. Invest Ophthalmol Vis Sci 16:771–774
15. Oldfield BJ, McLachlan EM (1977) Uptake and retrograde transport of HRP by axons of intact and damaged peripheral nerve trunks. Neurosci Lett 6:135–141
16. Putting BJ, Zweypfenning RCVJ, Vrensen GFJM, Oosterhuis JA, Van Best JA (1992) Dysfunction and repair of the blood retina barrier following white light exposure. A fluorophotometric and histologic study. Exp Eye Res 54:133–141
17. Robinson SR, Dreher Z (1990) Müller cells in adult rabbit retinas: morphology, distribution and implications for function and development. J Comp Neurol 292:178–192
18. Schwartz JH (1979) Axonal transport: components, mechanisms, and specificity. Annu Rev Neurosci 2:467–504
19. Steinberg RH, Schmidt R, Brown KT (1970) Intracellular responses to light from cat pigment epithelium: origin of the electroretinogram C-wave. Nature 227:728–730
20. Tso MOM, Woodford BJ (1983) Effect of photic injury on retinal tissues. Ophthalmology 90:952–963
21. Van den Pol AN, Decavel C (1990) Synaptic interactions of chemically defined neurons. In: Handbook of chemical neuroanatomy, vol 8: Analysis of neuronal microcircuits and synaptic interactions. Elsevier, Amsterdam New York Oxford, pp 199–271